Playa del Rey, California
InSAR Ground Deformation Monitoring
Final Report

Ref.: RV-14524
Doc.: CM-089-02
November 8, 2013

GEOSPATIAL SERVICES

SUBMITTED TO:

Southern California Gas Company
555 W. Fifth Street (Mail Location 23E2)
Los Angeles, CA, USA
90013-1041

ATTN: Mr. Rick Gailing

SUBMITTED BY:

MDA Geospatial Services
57 Auriga Drive, Suite 201
Ottawa, Ontario K2E 8B2
CANADA

Tel: +1-613-727-1087
Fax: +1-613-727-5853

Prepared By:	________________ Mary Anne McParland Remote Sensing Analyst	November 8, 2013
Reviewed By:	________________ Shinya Sato Sr. Remote Sensing Analyst	November 8, 2013
Reviewed By:	________________ Gillian Robert Sr. Project Manager	November 8, 2013

Executive Summary

This final report, describes the concluding results and methodology used to monitor, as well as quantify the ground surface deformation at the Southern California Gas Company (SoCalGas) Playa del Rey Gas Storage Field by means of interferometric synthetic aperture radar (InSAR) satellite.

This five year program, May 2008 to June 2013, was established to monitor the vertical ground deformation within SoCalGas area of interest (AOI) using InSAR, capable of detecting changes in surface within a few millimeters. During this program, RADARSAT-2 imagery was used for the generation of vertical deformation maps over the AOI, two of which were delivered to SoCalGas every 6 months during that period.

The following summarizes the overall findings for the 5 year program as well as the results for the latest 6 month interval:

- RADARSAT-2 Ultra-fine ascending 3 meter resolution radar satellite data were acquired from May 2008 to June 2013.
- A total of 70 RADARSAT-2 images were used during the monitoring period. By enhancing the temporal and spatial accuracy, the use of repeated measurements has reduced the atmospheric noise and highlighted the fact that actual ground measurements in the Playa del Rey Gas Storage Field has been minimal in the last 5 years.
- During this time period however, the Playa del Rey Gas Storage Field area did experience large seasonal variations. These variations are reflected in the ground changes measured and are based on soil moisture primarily.

For the last 6 month interval:

- RADARSAT-2 Ultra-fine ascending satellite radar data were scheduled, acquired and analyzed from December 2012 to June 2013.
- The highest quality deformation maps are generated and include the time periods from December 2012 to March 2013 (Pair A) and March 2013 to June 2013 (Pair B).
- The delivered products are geo-referenced with a horizontal accuracy better than 20 ft. Areas of insufficient quality are masked out in the final products. The measurements in the AOI are of good quality.

- The estimated precision for the December 2012 to March 2013 vertical deformation product is 0.012 ft with a 95% confidence interval; while the estimated precision for the March 2013 to June 2013 vertical deformation product is 0.012 ft with a 95% confidence interval.
- For this sixth month time period, no significant deformation patterns can be detected within the SoCalGas AOI.
- The variation in the reported InSAR ground surface movement is likely related to soil moisture changes. The majority of this variance is within the reported noise level measurement of 0.02 ft.

Contents

List of Figures

List of Tables

List of Acronyms

AOI area of interest

InSAR interferometric synthetic aperture radar

SoCalGas Southern California Gas Company

1 Objective

The objective of this final report, is to provide SoCalGas with measurements of the ground deformation that occurred within the project's area of interest (AOI) using conventional interferometric synthetic aperture radar (InSAR) monitoring from December 2012 to June 2013 as well as conclude the five year monitoring program. For this final Milestone, two conventional InSAR deformation maps quantifying ground movement are generated.

This deliverable pertains to the tenth and final deliverable, Milestone 10, of a five year InSAR Monitoring Program, as described in Section 2.1 table 1 Milestone Deliverables of the Master Document. The five year program identifies areas where ground motion patterns are during each milestone period.

The InSAR ground deformation estimation methods implemented in this milestone reflect the procedures outlined in the Master Report of this monitoring program.

1.1 Report Organization

This report is organized as follows:

- Section 1 provides the introduction and report organization. This section also describes the AOI and the available data for the current monitoring time period.
- Section 2 describes the results for the deformation maps and includes the results of the cumulative vertical deformation products.
- Section 3 provides a summary and conclusions of this milestone and the overall five year program.
- Appendix A lists the deliverables provided for this last milestone.
- Appendix B includes all results measured during this five year program.
- Appendix C provides a list of definitions for commonly used terms.

1.2 Study Area

The Playa del Rey Gas Storage Field AOI and surrounding area, in Los Angeles, California, is shown in figure 1. The coordinates for the AOI interest are 34°01'58"N 118°28' 5"W and 33°56' 56"N 118°20'4"W. The area is predominantly flat.

MDA

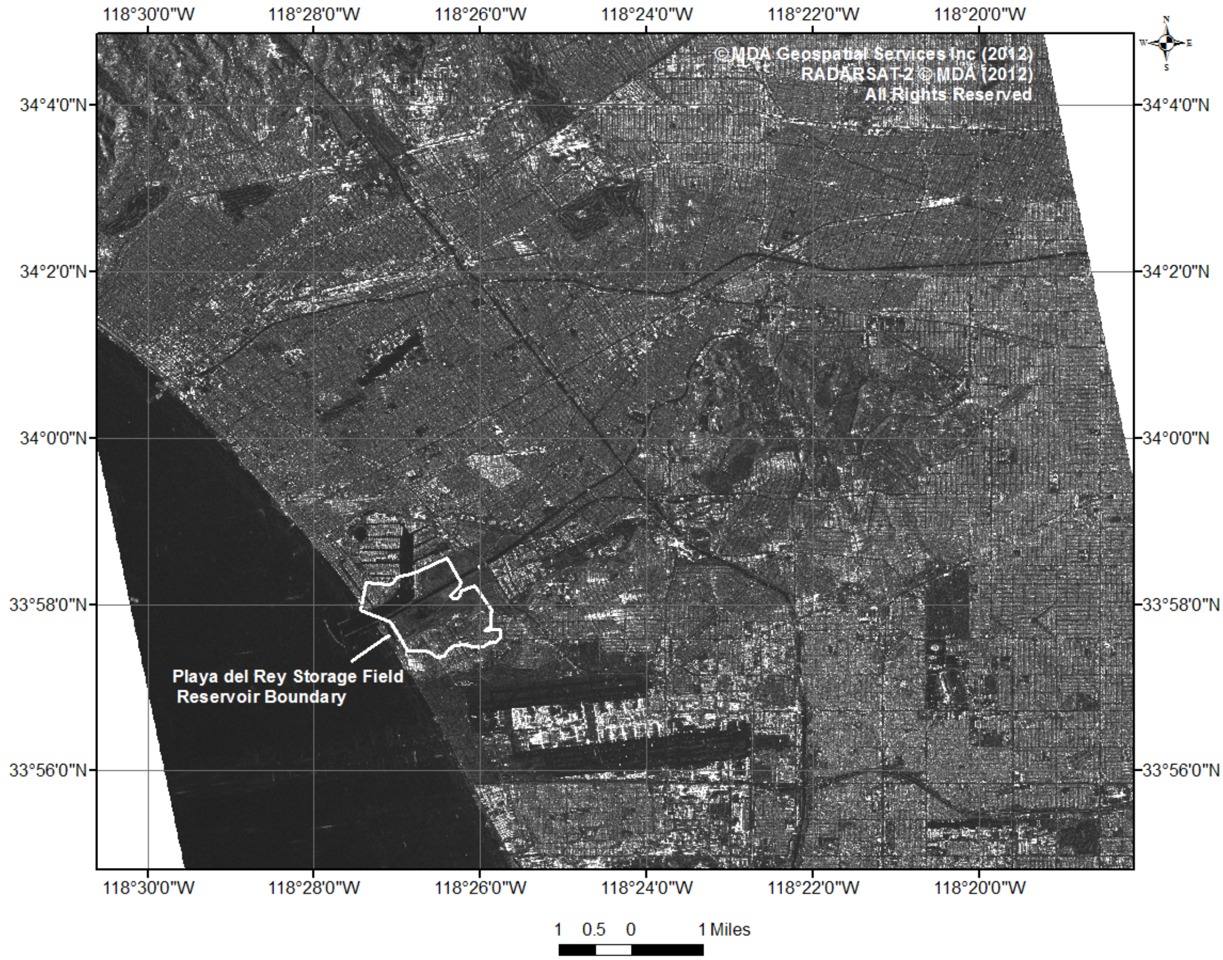

Figure 1: Playa del Rey AOI and surrounding area in Los Angeles.

1.3 Data Selection

The RADARSAT-2 Ultra-Fine data used to generate the deliverables for the December 2012 to June 2013 time period are listed in table 1 below. Also included are a full listing of the data from the onset of the monitoring program.

Table 1: RADARSAT-2 Ultra-Fine data acquired over Playa del Rey Gas Storage Field

Acquisition #	Acquisition Date	Acquisition #	Acquisition Date	Acquisition #	Acquisition Date
1	May 27, 2008	26	June 10, 2010	51	March 19, 2012
2	August 7, 2008	27	July 4, 2010	52	April 12, 2012
3	August 31, 2008	28	July 28, 2010	53	May 6, 2012
4	November 11, 2008	29	August 21, 2010	54	May 30, 2012
5	December 5, 2008	30	September 14, 2010	55	June 23, 2012
5	December 29, 2008	31	October 8, 2010	56	July 17, 2012
6	January 22, 2009	32	November 1, 2010	57	August 10, 2012
7	March 11, 2009	33	November 25, 2010	58	September 3, 2012
9	April 4, 2009	34	December 19, 2010	59	September 27, 2012
10	April 28, 2009	35	January 12, 2011	60	October 21, 2012
11	May 22, 2009	36	February 5, 2011	61	November 14, 2012
12	June 15, 2009	37	March 1, 2011	62	December 8, 2012
13	July 9, 2009	38	March 25, 2011	63	January 1, 2013
14	August 2, 2009	39	April 18, 2011	64	January 25, 2013
15	August 26, 2009	40	May 12, 2011	65	February 18, 2013
16	September 19, 2009	41	June 5, 2011	66	March 14, 2013
17	October 13, 2009	42	June 30, 2011	67	April 7, 2013
18	November 6, 2009	43	August 16, 2011	68	May 1, 2013
19	November 30, 2009	44	September 9, 2011	69	May 25, 2013
20	December 24, 2009	45	October 3, 2011	70	June 18, 2013
21	January 17, 2010	46	October 27, 2011		
22	February 10, 2010	47	November 20, 2011		
23	March 6, 2010	48	December 14, 2011		
24	March 30, 2010	49	January 31, 2012		
25	May 17, 2010	50	February 24, 2012		

The InSAR deformation maps created for the last six month time period are listed in table 2.

Table 2: Selected RADARSAT-2 data for the InSAR analysis. The pairing numbers refer to the acquisition numbers from table 1.

Interferogram Pair	**Acquisition Date Master**	**Acquisition Date Slave**
A (1-5)	Dec-8-12	Mar-14-13
B (5-9)	Mar-14-13	Jun-18-13

2 Results - Interim Report I

An analysis of the available data is carried out by evaluating all possible interferometric combinations. Two InSAR pairs are selected for the generation of deformation products:

- Pair A for the time period between December 8, 2012 to March 14, 2013 (96 days)
- Pair B for the time period between March 14, 2013 to June 18, 2013 (96 days)

The root-mean-square of the observed values in the non-deformation area is indicative of the precision of the deformation map. To obtain a 95% confidence interval a factor of two is used. Table 3 and table 4 show the summary of the estimation of noise level for Pairs A and B, respectively.

Table 3: Summary for Pair A

Date	Time Span	Noise Level standard deviation [ft]	95% Confidence interval [ft]
Dec-8-12 to Mar-14-13	96 days	0.006	0.012

Table 4: Summary for Pair B

Date	Time Span	Noise Level standard deviation [ft]	95% Confidence interval [ft]
Mar-14-13 to Jun-18-13	96 days	0.006	0.012

Additional products, the cumulative vertical deformation, are presented in this report:

- Pair C for the time period between December 8, 2012 to June 18, 2013 (192 days)
- Pair D for the time period between May 27, 2008 to June 18, 2013 (1848 days)

The following sections present the results for both pairs A and B.

2.1 Pair A - December 8, 2012 to March 14, 2013

The vertical ground deformation in the Playa del Rey Gas Storage Field is observed for the time period between December 8, 2012 to March 14, 2013, as shown in figure 2.

The color representation of the vertical deformation product are shown in figure 3 and figure 4 after masking areas that contain noise. The estimated precision for Pair A is within ±0.012 ft with a 95% confidence interval.

A localized area of very subtle ground surface movement is observed in the AOI, in the easterly limits of the Playa del Rey Storage Field Reservoir Boundary, (center co-ordinate 33°58'00"'N 118°26'07"W) and likely related to higher amount of rainfall accumulated between this period, as recorded by the National Weather Service at LAX in table 5. The deformation values range from 0.02 to 0.03 ft of uplift, as shown in figure 3. No significant subsidence is seen in the Playa del Rey Gas Storage field from December 2012 to March 2013.

Similar patterns of uplift were also observed in Milestone E, monitoring period December 19, 2010 to March 1, 2011, where deformation values range from 0.03 to 0.04 ft of uplift, as shown in Appendix B, figure 22.

Table 5: Rainfall accumulation per month at LAX. Source: National Weather Service.

Month	Monthly Precipitation [inches]	Month	Monthly Precipitation [inches]
June 2009	0.15	January 2012	1.19
July 2009	0.00	February 2012	0.12
August 2009	0.00	March 2012	1.78
September 2009	Trace	April 2012	1.51
October 2009	1.31	May 2012	0.01
November 2009	0.00	June 2012	0.00
December 2009	2.05	July 2012	Trace
January 2010	6.01	August 2012	Trace
February 2010	4.55	September 2012	Trace
March 2010	0.21	October 2012	0.12
April 2010	1.25	November 2012	0.77
May 2010	0.00	December 2012	1.91
June 2010	0.00	January 2013	1.30
July 2010	Trace	February 2013	0.20
August 2010	0.00	March 2013	0.66
September 2010	Trace	April 2013	0.06
October 2010	1.56	May 2013	0.39
November 2010	0.59	June 2013	0.00
December 2010	8.83		
January 2011	0.81		
February 2011	1.47		
March 2011	4.04		
April 2011	Trace		
May 2011	0.53		
June 2011	0.02		
June 2011	0.02		
July 2011	Trace		
August 2011	0.00		
September 2011	0.01		
October 2011	0.63		
November 2011	1.69		
December 2011	0.67		

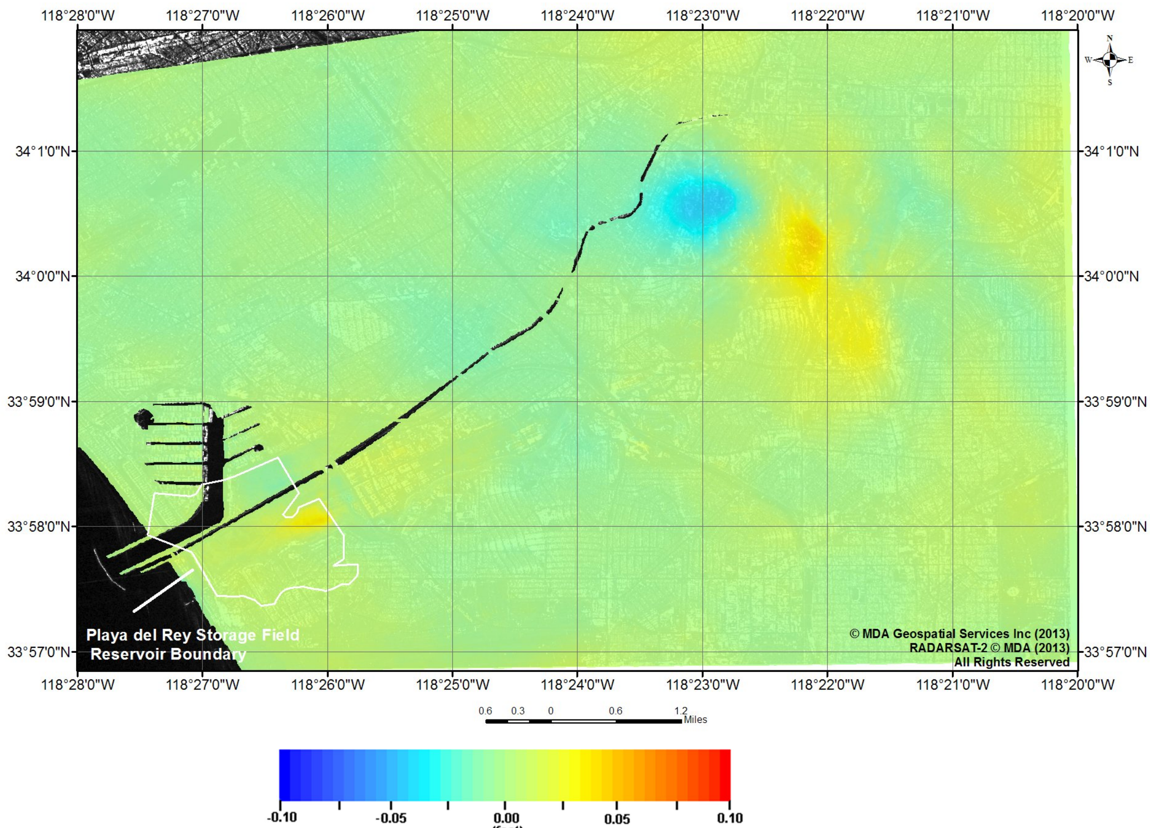

Figure 2: Playa del Rey Gas Storage Field AOI and surrounding area. Color representation of the vertical deformation product from December 8, 2012 to March 14, 2013 superimposed on SAR image without contours. In this representation, blue corresponds to subsidence and red indicates uplift.

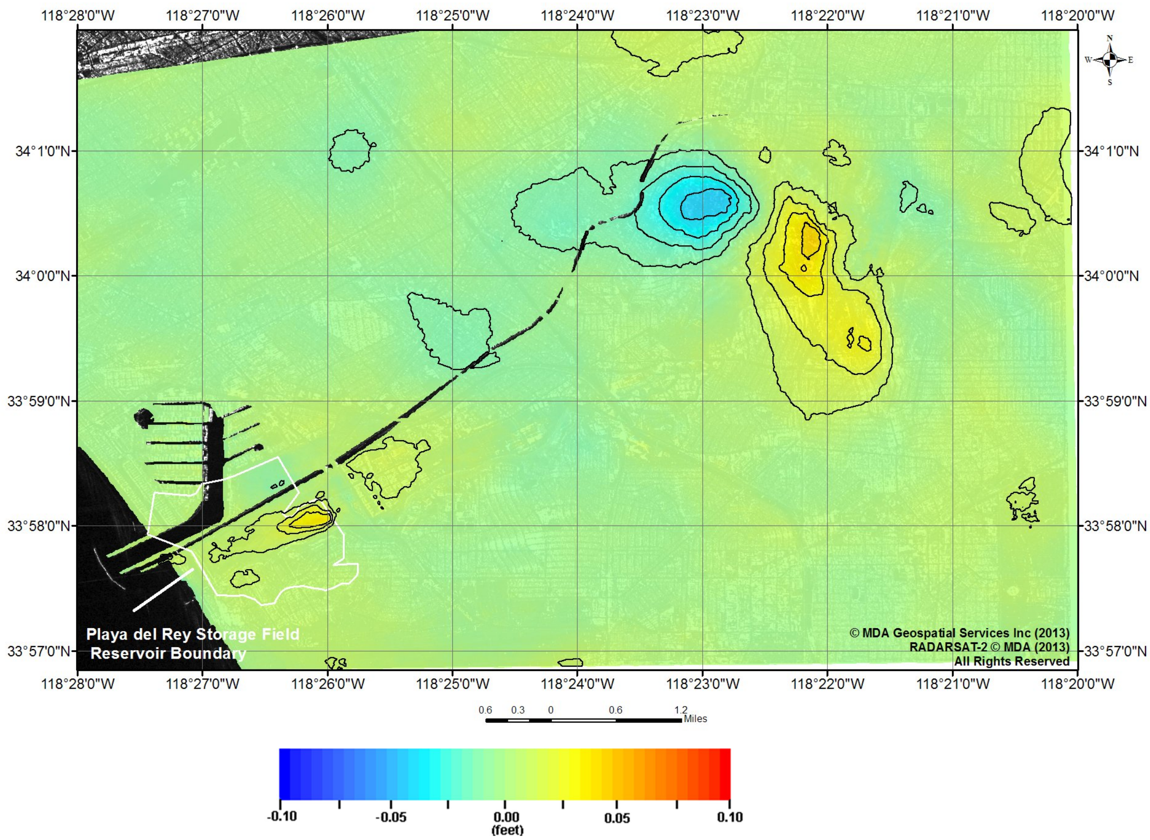

Figure 3: Playa del Rey Gas Storage Field AOI and surrounding area. Color representation of the vertical deformation product from December 8, 2012 to March 14, 2013 superimposed on SAR image with 0.01 ft contours. In this representation, blue corresponds to subsidence and red indicates uplift.

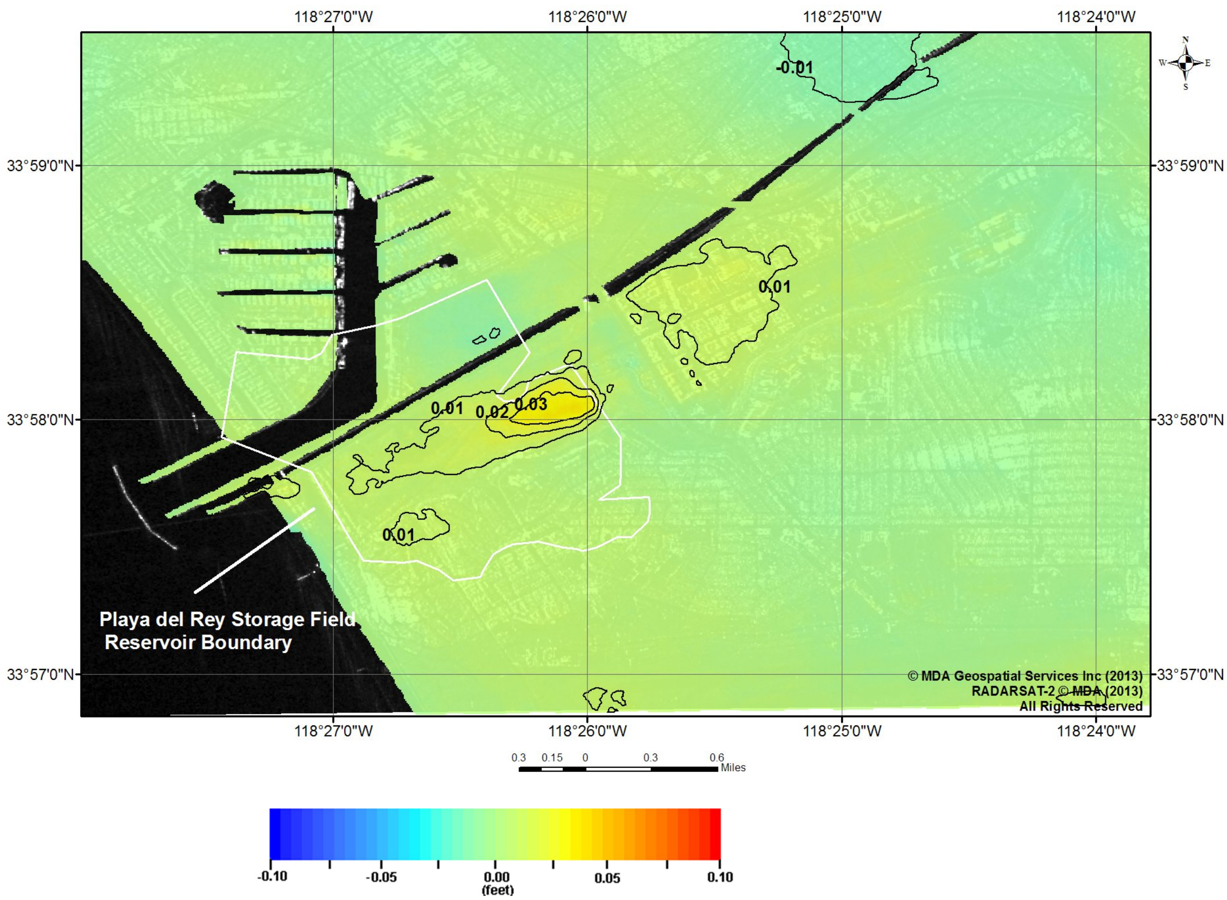

Figure 4: Zoom-in of Playa del Rey Gas Storage Field AOI. Color representation of the vertical deformation product from December 8, 2012 to March 14, 2013 superimposed on SAR image with 0.01 ft contours. In this representation, blue corresponds to subsidence and red indicates uplift.

2.2 Pair B - March 14, 2013 to June 18, 2013

The vertical ground deformation in the Playa del Rey Gas Storage Field is observed for the time period between March 14, 2013 to June 18, 2013, as shown in figure 5.

Figure 6 and figure 7 present a color representation of the final product. The estimated precision for Pair B is within $\pm$0.012 ft with a 95% confidence interval.

A localized area of deformation is observed in the AOI, in the easterly limits of the Playa del Rey Storage Field Reservoir Boundary, (center co-ordinate 33°58'18"'N 118°25'57"W). Subtle deformation values range from 0.02 to 0.04 ft subsidence, as shown in figure 7.

As was observed with Pair A, a similar pattern of subsidence was also observed in Milestone E, Appendix B, figure 23.

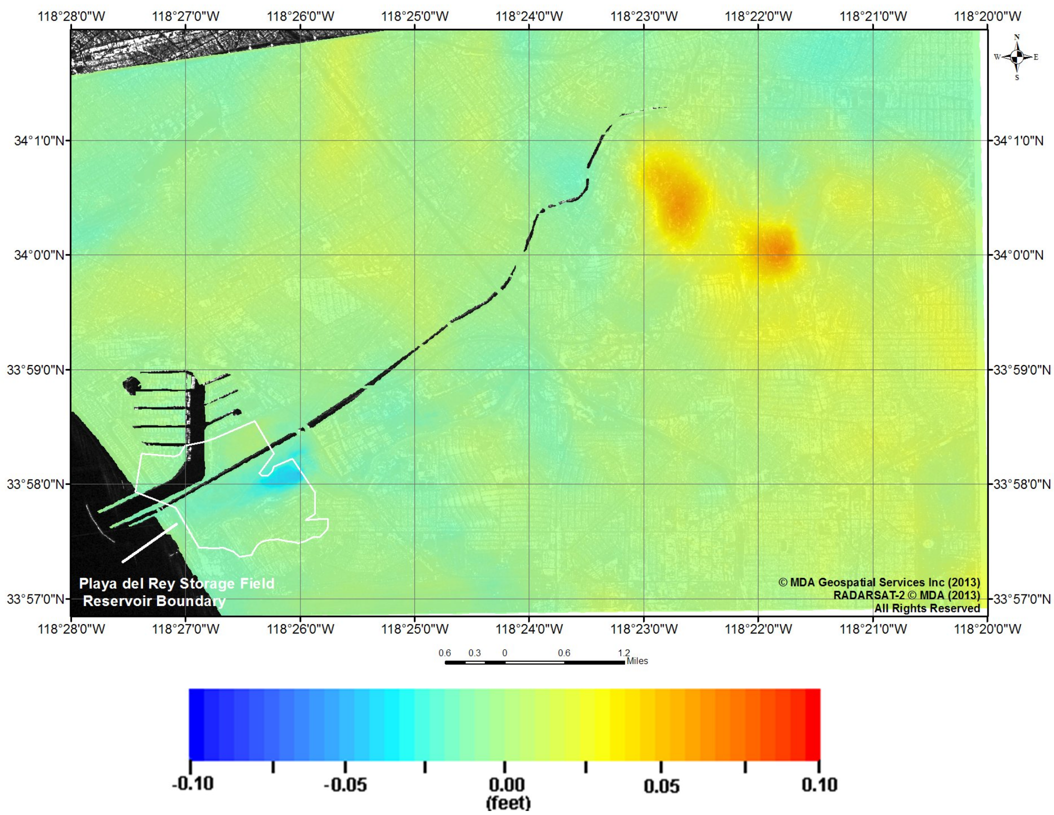

Figure 5: Playa del Rey Gas Storage Field AOI and surrounding area. Color representation of the vertical deformation product from March 14, 2013 to June 18, 2013 superimposed on SAR image without contours. In this representation, blue corresponds to subsidence and red indicates uplift.

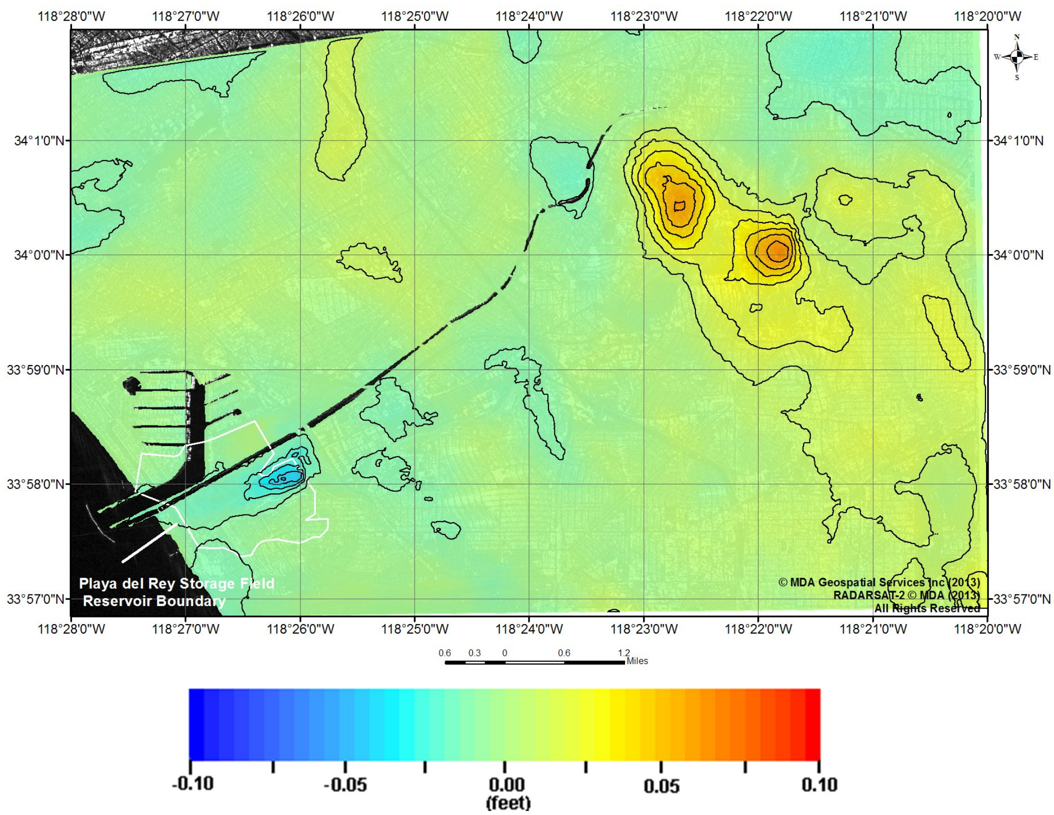

Figure 6: Playa del Rey Gas Storage Field AOI and surrounding area. Color representation of the vertical deformation product from March 14, 2013 to June 18, 2013 superimposed on SAR image with 0.01 ft contours. In this representation, blue corresponds to subsidence and red indicates uplift.

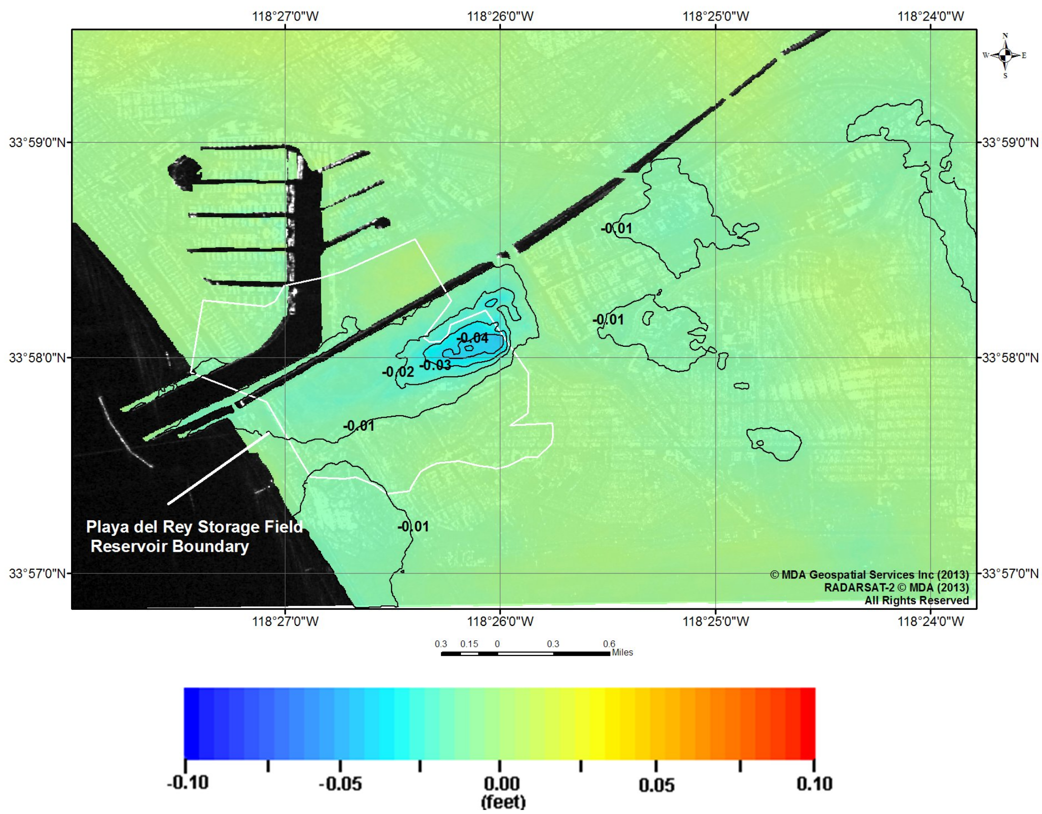

Figure 7: Zoom-in of Playa del Rey Gas Storage Field AOI and surrounding area. Cumulative vertical deformation from March 14, 2013 to June 18, 2013, with 0.01 ft contours.

2.3 Pair C - Cumulative Vertical Deformation December 8, 2012 to June 18, 2013

Pair C represents the cumulative vertical deformation results over the AOI and surrounding areas in Los Angeles from December 2012 to June 2013 (figure 8).

By enhancing the temporal and spatial accuracy, the use of repeated measurements has reduced the atmospheric noise and highlighted the fact that the actual ground movement in the Playa del Rey Gas Storage Field is negligible and related to phase and atmospheric noise (figure 9).

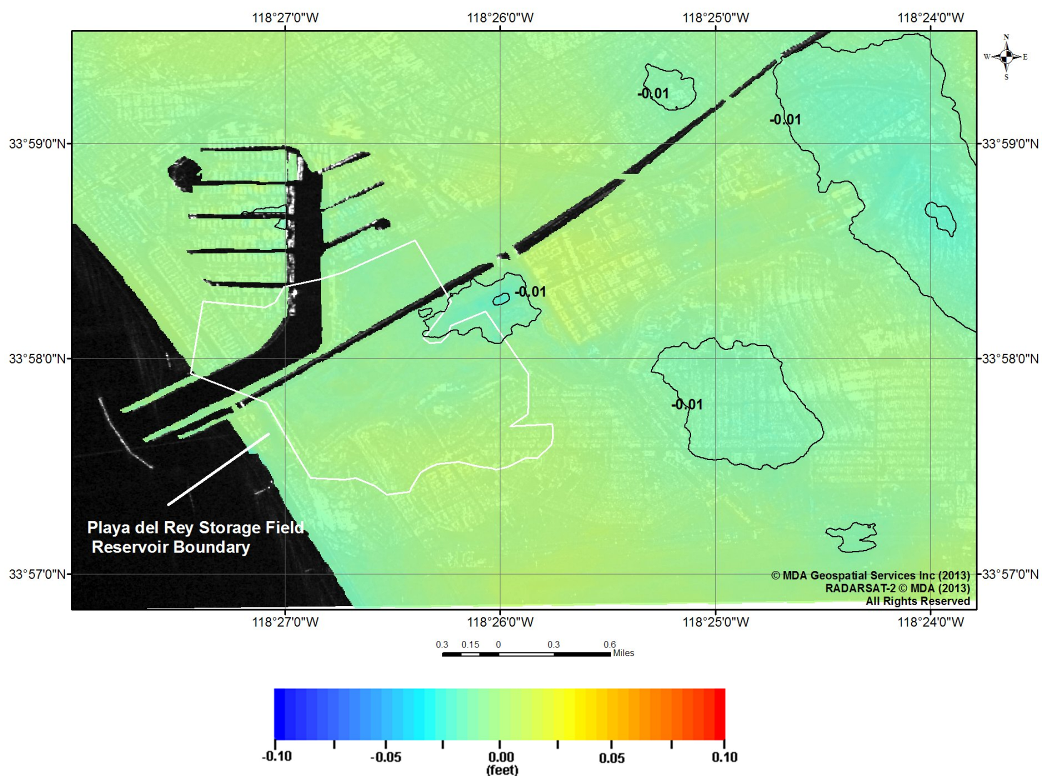

Figure 8: Playa del Rey Gas Storage Field AOI and surrounding area. Color representation of the cumulative vertical deformation from December 8, 2012 to June 18, 2013 superimposed onto SAR image.

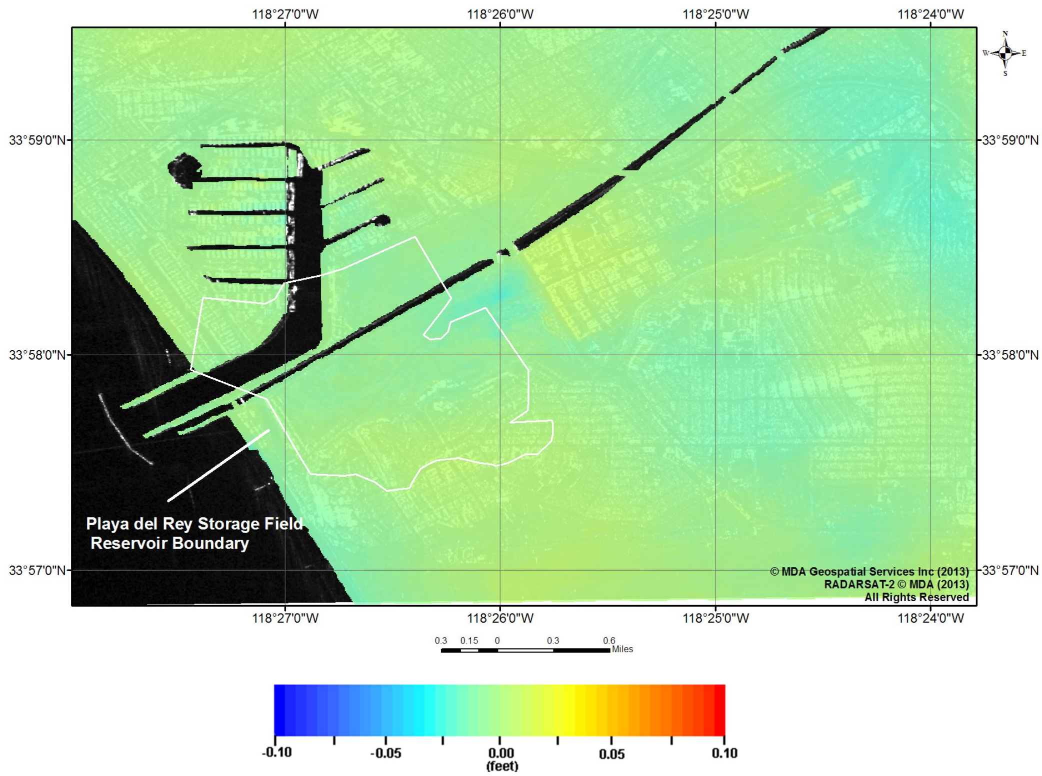

Figure 9: Zoom-in of Playa del Rey Gas Storage Field. Color representation of the summation of the vertical deformation products from December 8, 2012 to June 18, 2013 superimposed on SAR image with 0.01 ft contours. In this representation, blue corresponds to subsidence and red indicates uplift.

2.4 Pair D - Cumulative Vertical Deformation May 27, 2008 to June 18, 2013

Pair D represents the cumulative vertical deformation results over the AOI from the start of the monitoring period, May 27, 2008 to the current period analyzed, June 18, 2013 as is shown in figure 10 and 11.

Minimal ground surface movement is observed in the Playa del Rey Gas Storage Field AOI over the 5 year time period. This result is attributed to natural terrain expansion and contraction during the time periods where surface moisture has fluctuated.

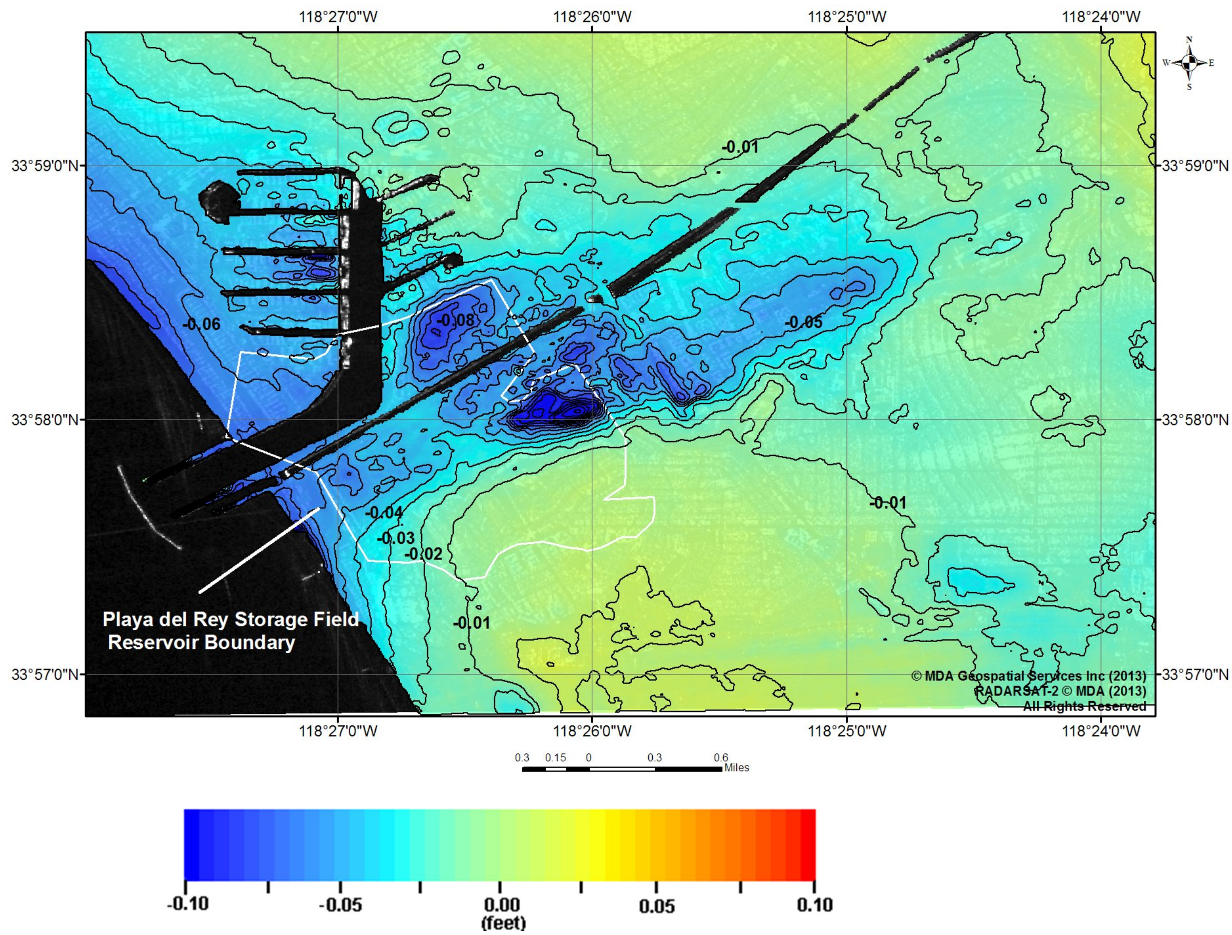

Figure 10: Zoom-in of Playa del Rey Gas Storage Field AOI and surrounding area. Cumulative vertical deformation from May 27, 2008 to June 18, 2013, with 0.01 ft contours.

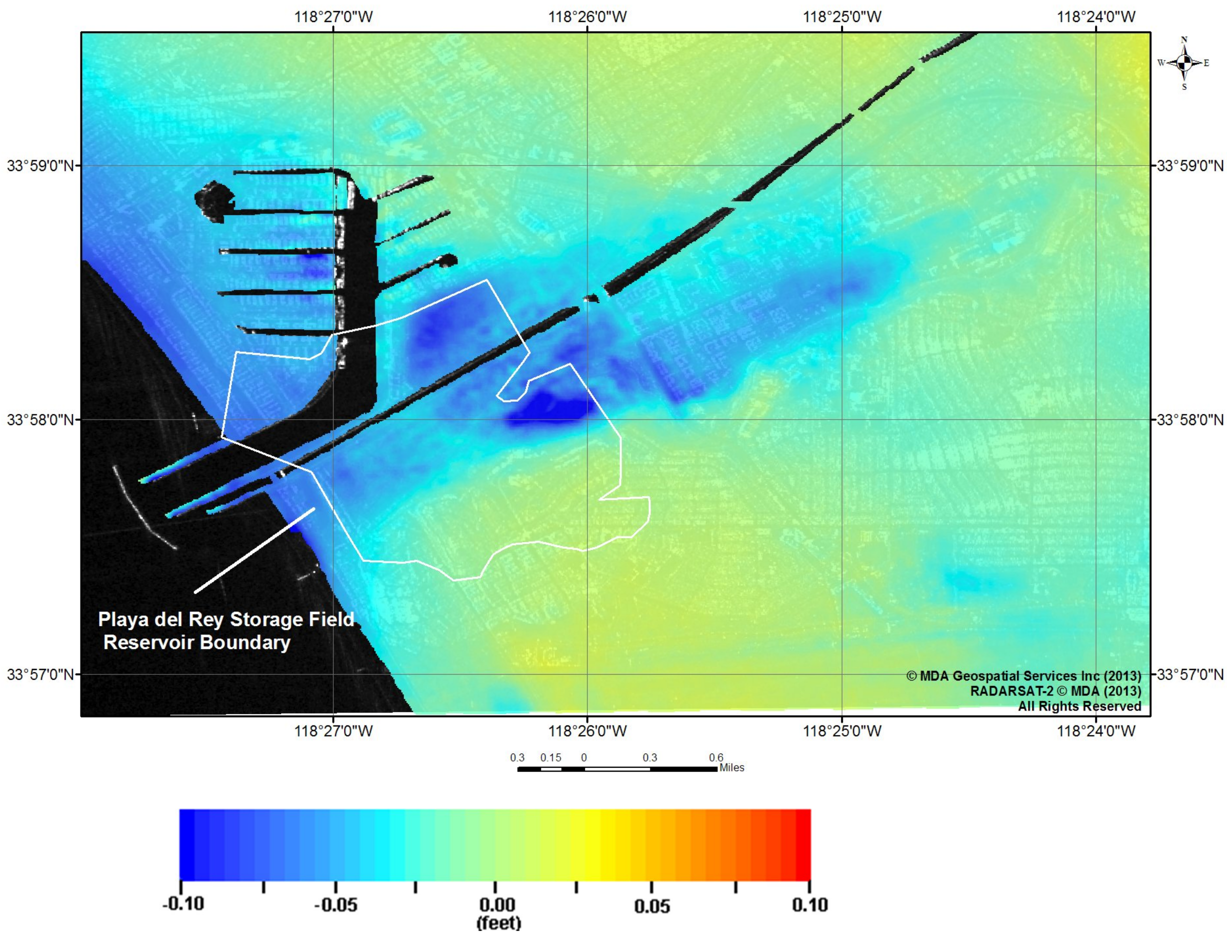

Figure 11: Playa del Rey Gas Storage Field AOI and surrounding area. Color representation of the cumulative vertical deformation from May 27, 2008 to June 18, 2013 superimposed onto SAR image.

3 Concluding Remarks

Vertical surface deformation measurements are derived for the Playa del Rey Gas Storage Field and surrounding areas in Los Angeles using conventional InSAR. This report, referred to as Interim Report I, pertains to final Milestone 10 of the current contract, RV-14524.

The following items describe the main findings of the work performed, for this milestone:

- RADARSAT-2 Ultra-Fine ascending data were scheduled by MDA for acquisition. The acquired data, covering the period of December 2012 to June 2013, were analyzed and utilized as part of the deliverable.
- Two deformation maps were generated. The estimated precision for the vertical deformation product Pair A, December 8, 2012 to March 14, 2013 is 0.012 ft with a 95% confidence interval. The estimated precision for Pair B, March 14, 2013 to June 18, 2013 is 0.012 ft with a 95% confidence interval.
- The variation in the reported InSAR ground surface movement to present is likely related to soil moisture changes. The majority of this variance is within the reported measurement of 0.02 ft, the noise level.
- The resulting analysis from December 2012 to June 2013, indicates that no major deformation pattern is occurring in the Playa del Rey Gas Storage Field.

In conclusion, the focus of the five year program was directed at detecting any ground movement with Playa del Rey Gas Storage Field. The findings from this long term program are:

- RADARSAT-2 provided good resolution and geometry of the Playa del Rey Gas Storage Field for InSAR monitoring.
- The area of interest experienced large variations in precipitation from winter to summer.
- Variation in the reported ground surface is likely due to soil moisture changes. It is anticipated that the majority of this variance is within the error measurement of 0.02 ft.
- By enhancing the temporal and spatial accuracy, the use of repeated measurements has reduced the atmospheric noise and highlighted the fact that actual ground measurements in the Playa del Rey Gas Storage Field is minimal.

A Deliverables

The deliverables, which are included on CD-ROM for Milestone 10, are listed in Table 6. These delivered data are described in XYZ ASCII files and are in California US State Plane, NAD27, 20 ft spacing.

Table 6: Delivered Data

Deliverable file	**Description**
PlayadelRey_SoCalGas_InterimReportI_2013.pdf	Interim Report I in PDF format.
Conventional Deformation map	
120812_031413_DEF.xyz 120812_031413_DEF.tif 031413_061813_DEF.xyz 031413_061813_DEF.tif	ASCII files with location and vertical deformation measurements in ft. Areas of low coherence are masked out with values set to -999.
Projection_Report.pdf	Describes the coordinate projection system of the delivered data.

B Playa del Rey

This section provides maps demonstrating spatially the historical vertical ground movement observed over the Playa del Rey region from May 2008 to December 2012.

Vertical deformation map products are shown in the following figures for the following time periods:

- Figure 12: Milestone 1, Master Report, May 27, 2008 to August 31, 2008
- Figure 13: Milestone 1, Master Report, August 31, 2008 to December 5, 2008
- Figure 14: Milestone 2, Interim Report A, December 5, 2008 to March 11, 2009
- Figure 15: Milestone 2, Interim Report A, March 11, 2009 to June 15, 2009
- Figure 16: Milestone 3, Interim Report B, June 15, 2009 to September 19, 2009
- Figure 17: Milestone 3, Interim Report B, September 19, 2009 to December 24, 2009
- Figure 18: Milestone 4, Interim Report C, December 24, 2009 to March 6, 2010
- Figure 19: Milestone 4, Interim Report C, March 6, 2010 to June 10, 2010
- Figure 20: Milestone 5, Interim Report D, June 10, 2010 to September 14, 2010
- Figure 21: Milestone 5, Interim Report D, September 14, 2010 to December 19, 2010
- Figure 22: Milestone 6, Interim Report E, December 19, 2010 to March 1, 2011
- Figure 23: Milestone 6, Interim Report E, March 1, 2011 to June 29, 2011
- Figure 24: Milestone 7, Interim Report F, June 29, 2011 to September 9, 2011
- Figure 25: Milestone 7, Interim Report F, September 9, 2011 to December 14, 2011
- Figure 26: Milestone 8, Interim Report G, December 14, 2011 to March 19, 2012

- Figure 27: Milestone 8, Interim Report G, March 19, 2012 to June 23, 2012
- Figure 28: Milestone 9, Interim Report H, June 23, 2012 to September 3, 2012
- Figure 29: Milestone 9, Interim Report H, September 3, 2012 to December 18, 2012.

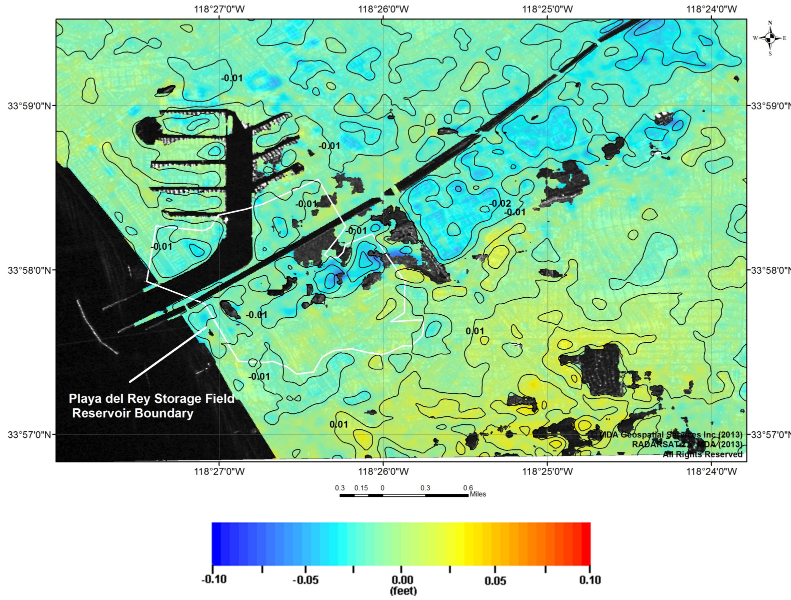

Figure 12: Vertical deformation from May 27, 2008 to August 31, 2008.

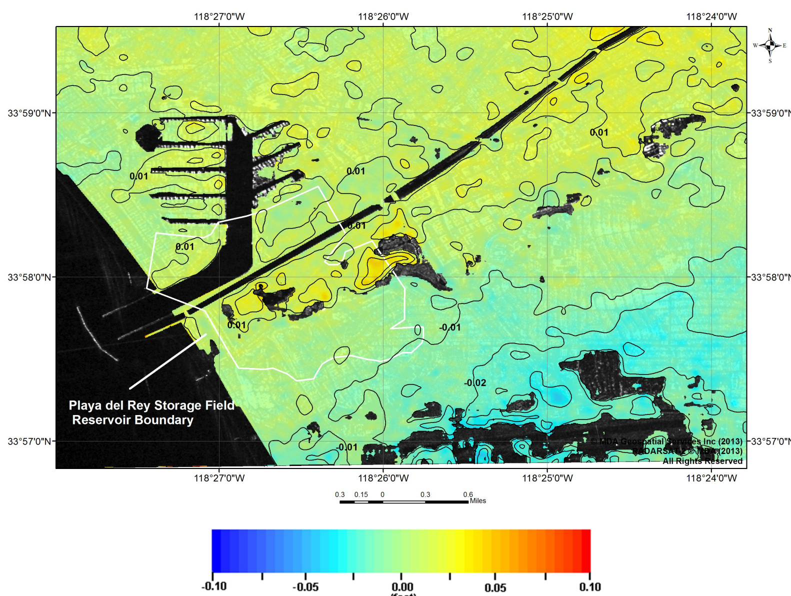

Figure 13: Vertical deformation from August 31, 2008 to December 5, 2008.

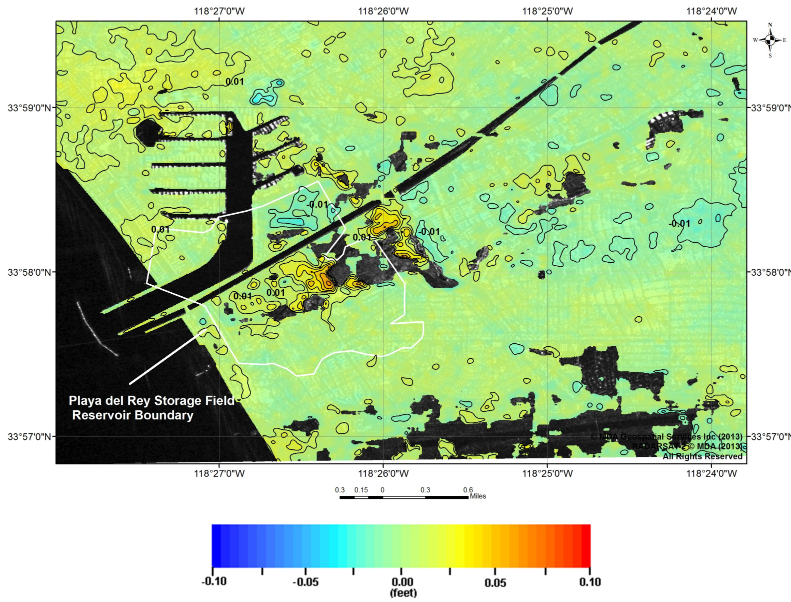

Figure 14: Vertical deformation from December 5, 2008 to March 11, 2009.

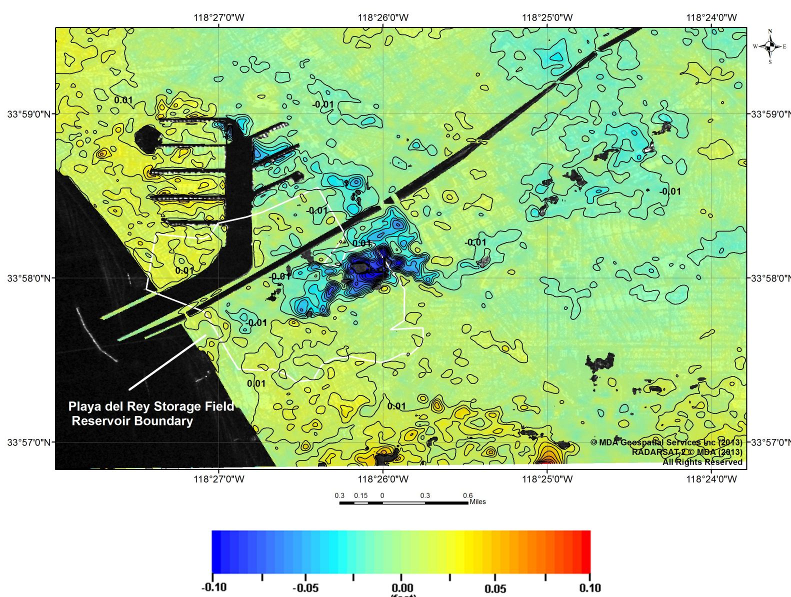

Figure 15: Vertical deformation from March 11, 2009 to June 15, 2009.

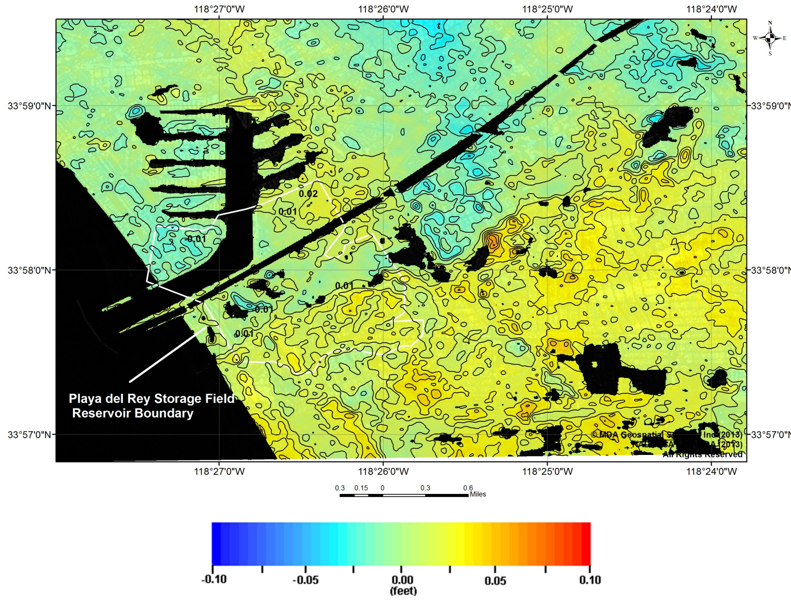

Figure 16: Vertical deformation from June 15, 2009 to September 19, 2009.

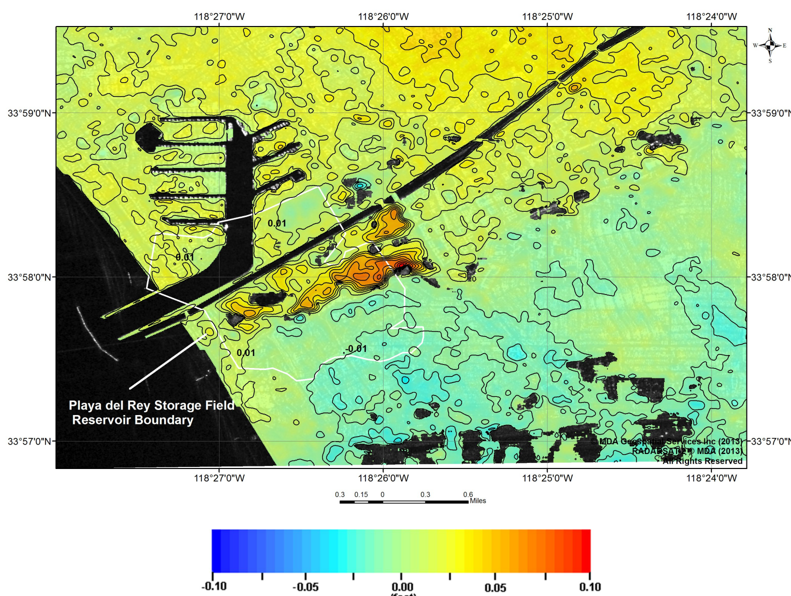

Figure 17: Vertical deformation from September 19, 2009 to December 24, 2009.

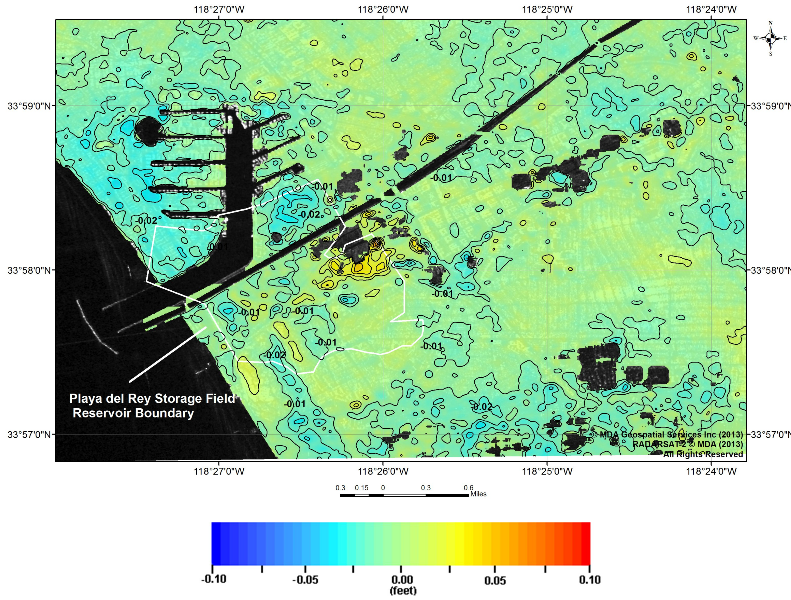

Figure 18: Vertical deformation from December 24, 2009 to March 6, 2010.

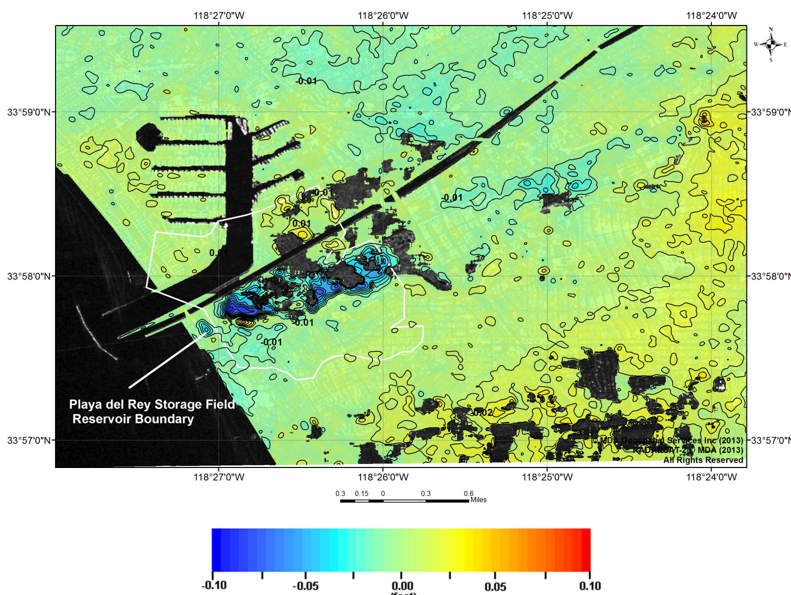

Figure 19: Vertical deformation from March 6, 2010 to June 10, 2010.

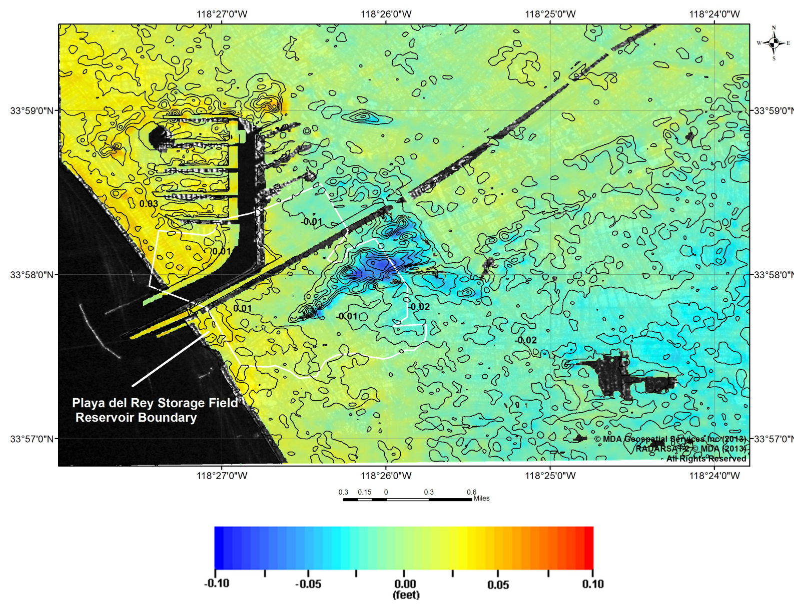

Figure 20: Vertical deformation from June 10, 2010 to September 14, 2010.

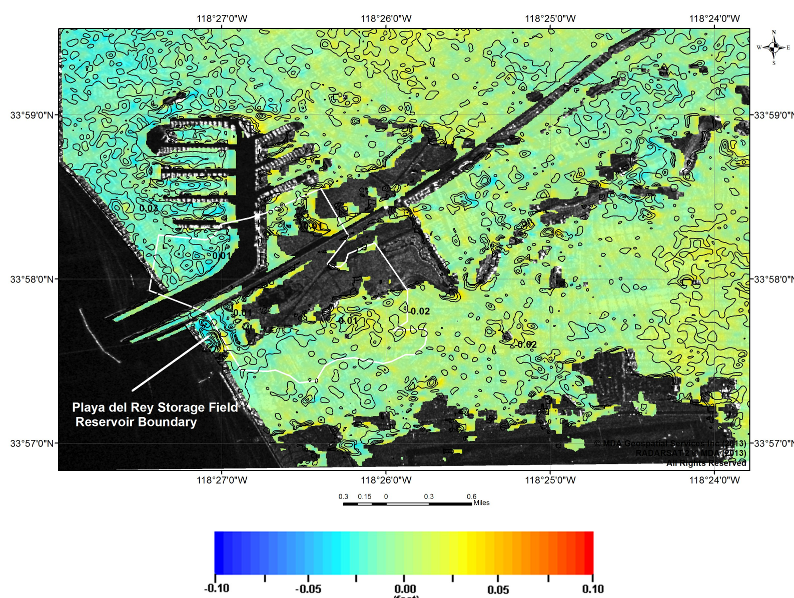

Figure 21: Vertical deformation from September 14, 2010 to December 19, 2010.

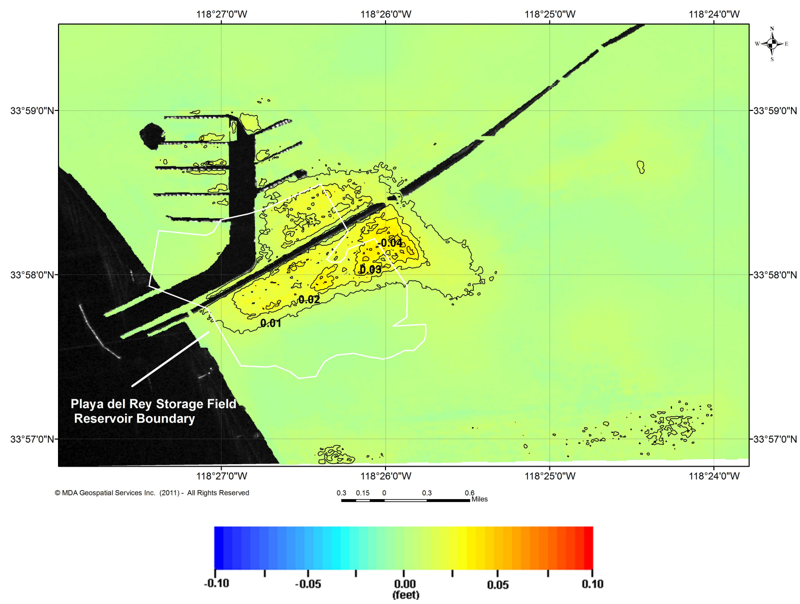

Figure 22: Vertical deformation from December 19, 2010 to March 1, 2011.

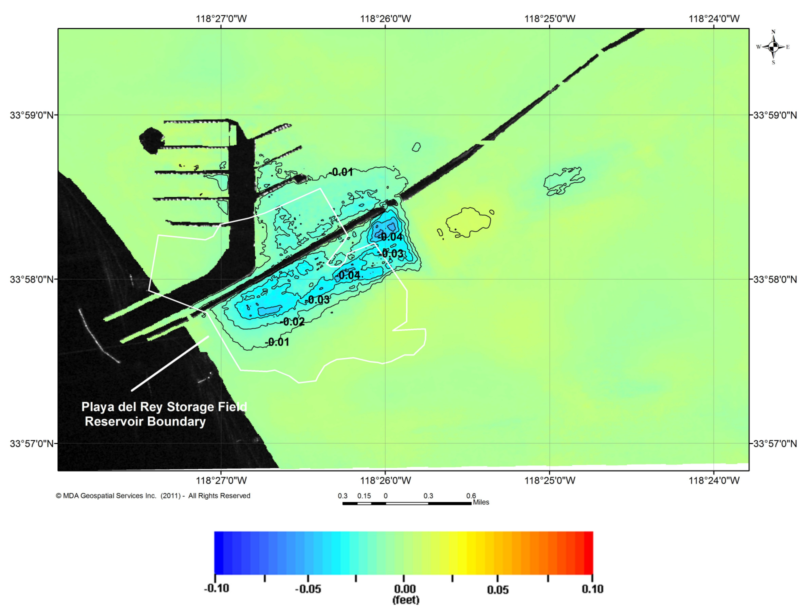

Figure 23: Vertical deformation from March 1, 2011 to June 29, 2011.

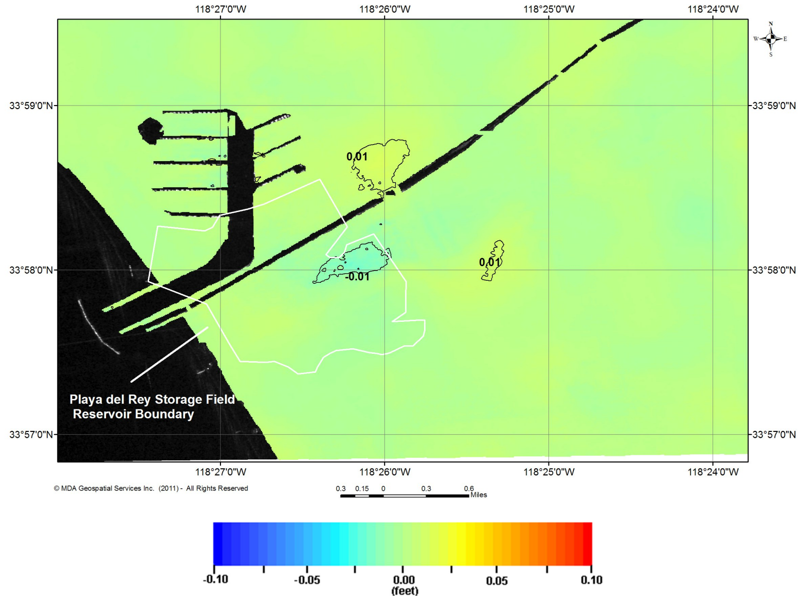

Figure 24: Vertical deformation from June 29, 2011 to September 9, 2011.

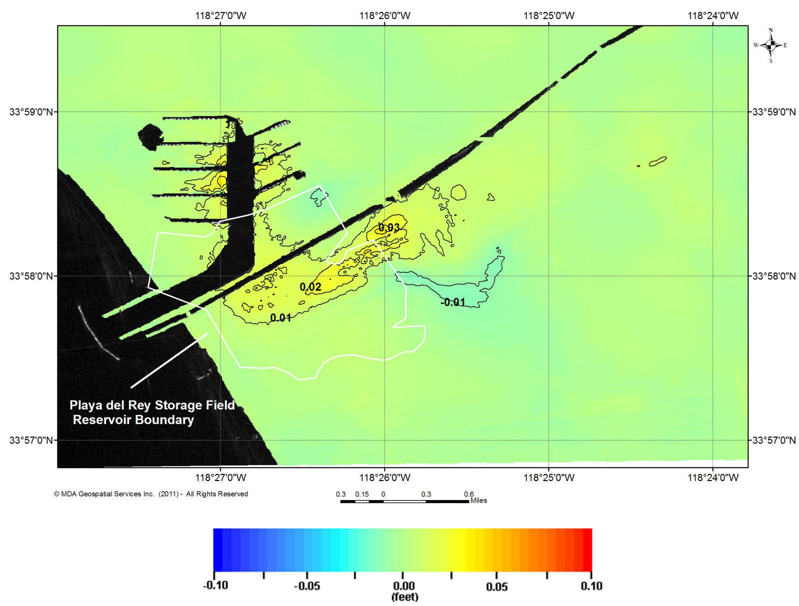

Figure 25: Vertical deformation from September 9, 2011 to December 14, 2011.

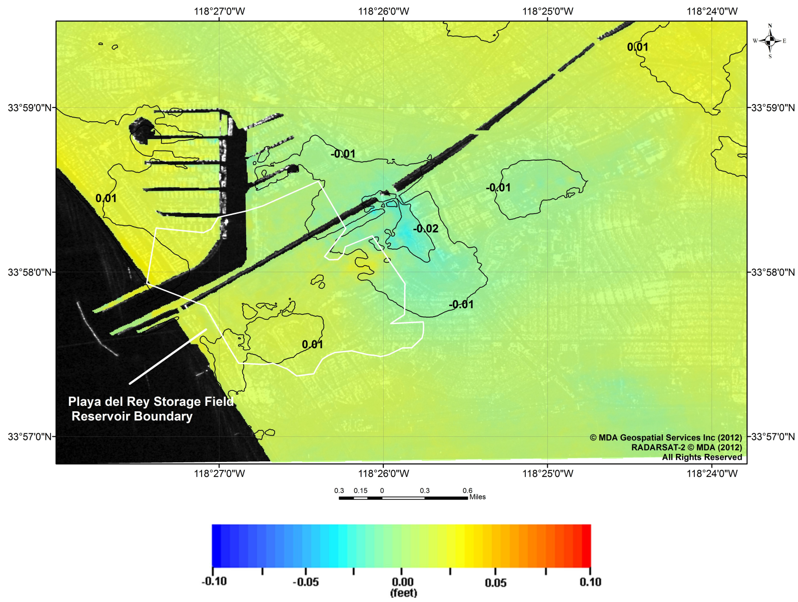

Figure 26: Vertical deformation from December 14, 2011 to March 19, 2012.

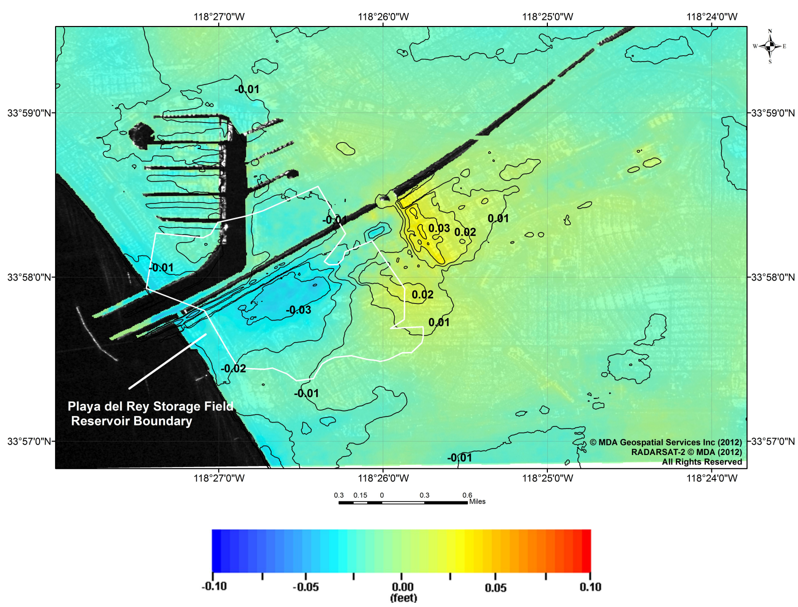

Figure 27: Vertical deformation from March 19, 2012 to June 23, 2012.

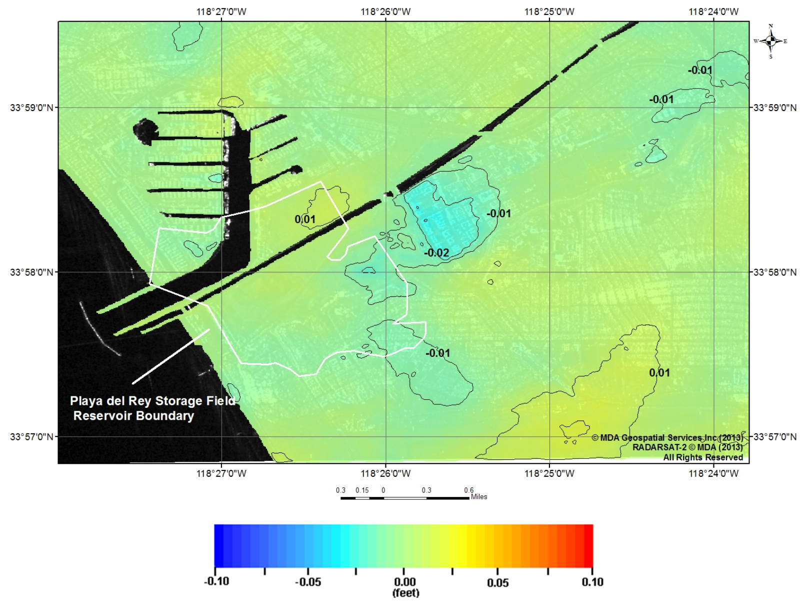

Figure 28: Vertical deformation from June 23, 2012 to September 3, 2012.

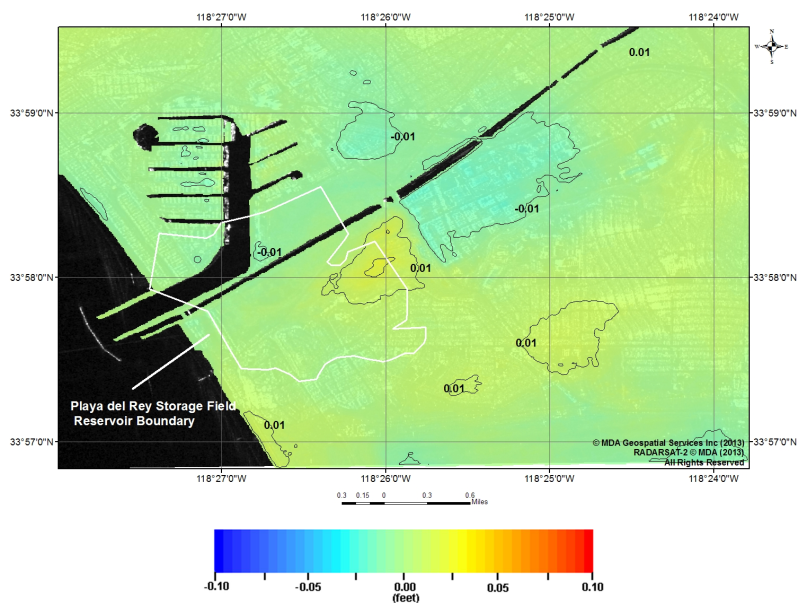

Figure 29: Vertical deformation from September 3, 2012 to December 8, 2012.

C Standard Definitions

Amplitude (a) The amplitude of a wave is the distance from the centre of the wave to the peak, see Figure 30.

Ascending Satellite tracks that transit from the south to the north are labeled ascending.

Aspect Angle (α) The aspect angle is the angle at which the local area is observed.

Azimuth Azimuth or track describes the direction of travel of the sensor over the ground.

Baseline (B) The baseline is the vector describing the distance between two radar observations of the same point (see also perpendicular baseline).

Coherence (γ) Coherence, γ, is used as a measure of the degree of similarity between the backscatter (amplitude and phase) response of coregistered SAR returns over time or space.

Coregistration Coregistration is the process of locating subsequent radar images to the same observation space. A set of coregistered images show information from the same point on the ground at the same image coordinate.

Descending Satellite tracks that transit from the north to the south are labeled descending.

Electromagnetic Wave An electromagnetic wave is a self-propagating wave that may exist in a vacuum or in matter. The wave has both electric and magnetic field components that oscillate with perpendicular phase. Electromagnetic radiation exists on a spectrum from gamma-rays to long radio waves. The visible spectrum is narrowly between 400 and 700 nm. Microwaves, the radiation used in SAR observations, are generally between a fraction of a millimetre and a metre in length.

Frequency (f) Frequency describes the number of cycles per second. Frequency is given in Hertz (Hz). For an electromagnetic wave, wavelength, λ, and frequency, f, are related through the speed of light, c, as $c = \lambda f$.

Frequency Band Radar frequencies are often referred to by a band letter. The coding goes back to the research conducted during WWII. C-Band extends from approximately 4-8 GHz. RADARSAT-1 & 2, ENVISAT, and ERS-1 & 2 all operate in C-Band. L-Band at 1-2 GHz was the operating frequency of the original SEASAT satellite in the 1970s, and the ALOS satellite currently operates in that range. The TerraSAR-X satellite operates in X-Band (8-12 GHz). Figure 31 shows the electromagnetic spectrum.

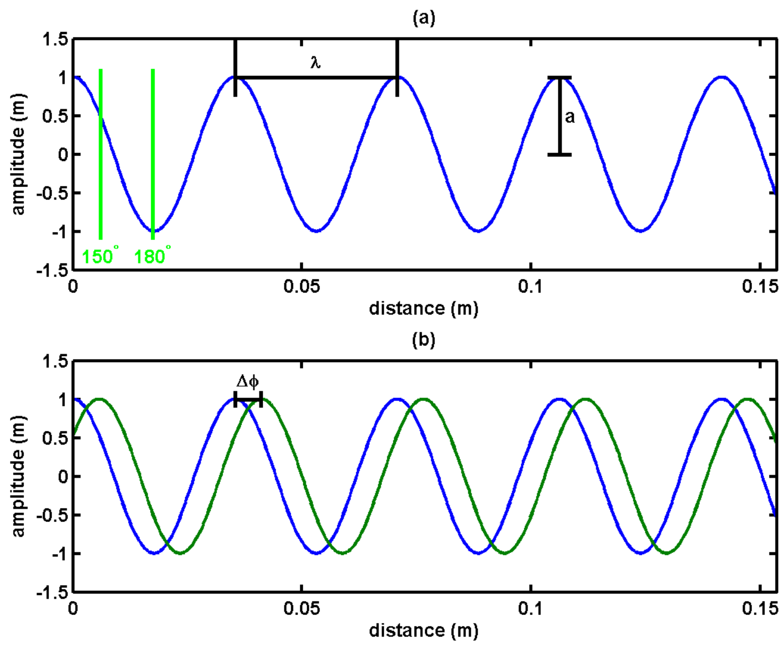

Figure 30: Definition of a 5.6-cm wave. Panel (a) shows the definition of wavelength, λ, and amplitude (a). The green lines show the location on the wave associated with 150° and 180° of phase. Panel (b) demonstrates the phase difference, $\Delta\phi$, between two waves.

Georeferencing Georeferencing is the procedure used to assign individual radar observations to geographic positions. The process involves calculating the geographic position based on the time to target and the observation time of the radar. Georeferencing for RADARSAT-2 has been measured (based only on the state vectors and the imaging geometry) to be better than 20 m on the ground.

Incident Angle (θ_i) The incident angle is the angle the incident radiation makes with respect to the surface normal. In satellite remote sensing, θ_i is often used to describe the angle between the mean surface normal and the incident radiation.

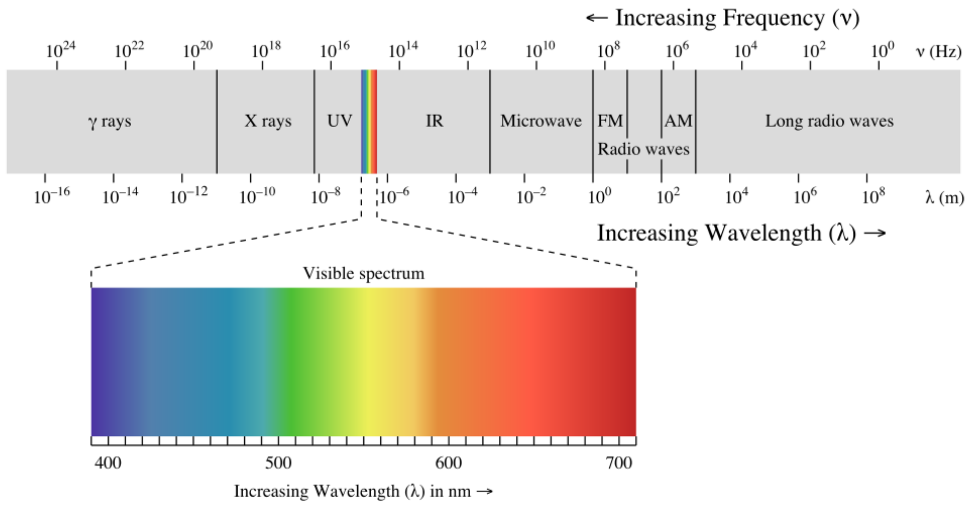

Figure 31: Electromagnetic spectrum showing the wavelength and frequency characteristics of radiation. The microwave portion of the spectrum contains the waves used for RADAR observation.

Line of Sight The line of sight describes travel of a wave from the radar to a point on the ground. Observations are only possible along the line of sight.

Look Direction Look direction refers to the side of the radar track (or azimuth) that the antenna pattern illuminates. That is, a right looking radar sends energy at approximately 90° to the right of the azimuth track.

Pass Pass or pass direction is used to refer to an ascending or descending satellite azimuth.

Perpendicular Baseline (B_{perp} or $B_{\perp}$) is the separation of two radar observations in the direction perpendicular to the first radar observation.

Phase (ϕ) Phase describes the position on a wave. Figure 30 shows a wave with phase labeled as 150° and 180°. ϕ is often reported in radians from 0 to 2π, which corresponds to degrees from 0 to 360.

Phase Difference ($\Delta\phi$) The phase difference (or phase shift) describes the difference between the position on two waves. Figure 30 shows a phase difference of 60° or $\pi/3$. The accuracy with which the phase difference can be measured is why InSAR is so valuable.

Phase Noise Phase noise refers to artifacts present in the phase measurement that are not due to the signal we want to capture.

Range (ρ or R) Range is used to describe the distance between a radar target on the ground and the sensor.

Slant Range Native SAR observations are recorded by time to target and time of observation. Slant range describes the distance along the radar line of sight.

Slant Range Coordinates The coordinate system of the native radar observations, defined by time of observation (azimuth) and time to target (slant range). Observations are aligned as range and azimuth pixels with constant spacing in slant range and slow time.

Speed of Light (c) The speed of light is 299,792,458 m/s.

Temporal Decorrelation As the time between observations increases, the physical reasons for the similarity of observations may change. In the monitoring of a field, for instance, the growth of grasses over time will cause decorrelation of the backscatter.

Wavelength (λ) Wavelength describes the distance between subsequent points of equal phase in consecutive cycles of a wave.